MEASUREMENT OF EFFECTIVE THERMAL CAPACITANCE IN BUILDINGS

K. Subbarao J. Burch E. Hancock H. Jeon

ABSTRACT

A short-term test method to measure the effective heat capacitance of a building is presented. The effective heat capacitance is defined in terms of the indoor temperature response to sinusoidal heat input; i.e., in terms of the thermal admittance. This definition is shown to yield a useful and measurable quantity, which can be related to a capacitance in a thermal circuit. A signal enhancement principle is introduced that allows accurate and repeatable measurements. The method is illustrated with data from a single family residence as well as a test cell. When additional mass was introduced into the test cell in the form of water containers, there was a well-determined change in admittance that agreed with expected change. Among the applications of this method are (1) diagnostics (measured versus calculated heat capacitance), and (2) a measurement-based characterization of heat capacitance effects of furnishings, for use in simulations.

INTRODUCTION

In assessing the dynamic response of a building, it is generally important to take into account the heat storage and release in the various building elements. If the interior temperature is maintained essentially a constant by space-conditioning equipment, the building heat capacitance plays only a minor role. Quite commonly, acceptable variations in inside temperature is a strategy to save energy as well as to reduce peak loads. Therefore, it is necessary to consider the effect of heat capacity of a building.

The main purpose of this paper is to present a short-term test method to accurately and repeatably measure the effective heat capacitance of a building "seen" by inside air. It is necessary to first define the effective heat capacitance, which is not quite as straightforward as it may seem at first glance. The definition should result in a useful and measurable quantity. For reasons that will become clear, the capacitance is defined in Section 2 through a certain admittance. Section 3 gives a discussion of issues in measuring the capacitance accurately and repeatably. In particular, a signal enhancement principle is introduced and the role of sinusoidal heat input is discussed. Section 4 gives experimental results from a single-family residence; Section 5 gives experimental results from a test cell that was tested with and without extra mass. Section 6 discusses the method and its implications. Section 7 has a summary and conclusions.

The work described here is part of a project to determine thermal characteristics of a building from short-term tests. These parameters are then used as inputs to an hour-by-hour simulation for a variety of applications (Subbarao 1984). The limited work reported in this article on the interior capacitance has broader applications. One planned application is to extract the response of furnishings in a building. This response can be converted into suitable response factors for use in simulations like DOE-2 and BLAST.

K. Subbarao and J. Burch are senior physicists, Buildings Research Branch, Solar Energy Research Institute, Golden, CO; E. Hancock is a consultant, Colorado Energy Associates, Fort Collins, CO; H. Jeon is a graduate student, Department of Civil, Environmental, and Architectural Engineering, University of Colorado, Boulder.

DEFINITION OF BUILDING CAPACITANCE

As noted in the Introduction, a definition of building capacitance that results in a useful and measurable quantity is an important issue. The sum of the capacitances of the individual building elements is only of very limited use since mass outside insulation (e.g., brick veneer), mass in thick walls (e.g., Trombe walls), and distributed mass (e.g., drywall) have very different roles in determining building performance.

One possible definition is through a cool-down test (Kelley et al. 1984). Suppose the building is maintained at a certain temperature above the ambient by a heat source, which is shut off at a certain time. If the test is done in the absence of solar and internal gains, the variations in infiltration are small enough, and the variations in the ambient temperature are small enough, the decay is a characteristic of the building capacitance. By fitting the decay to an exponential, a time constant can be determined. If the building capacitance is adequately modeled by the circuit of Figure 1, the time constant is given by (C/L) (1 + L/U). Knowing L and U (or only L, if L/U is small enough), the capacitance C can be determined. There are several limitations to this approach. One is that, except for relatively light buildings with well-distributed masses, the decay cannot be represented by a single exponential, but by a sum of exponentials. As a result, the single time constant obtained by a fit depends on the choice of the region of the decay curve. A second limitation is the variations in ambient temperature, etc. This can be accounted for by employing a regression technique rather than fitting to an exponential (Sonderegger 1978).

The circuit of Figure 1 is subject to the following pitfall: If the exterior walls are relatively massive, the circuit of Figure 1 is a poor representation of the building. The regression usually gives a good fit, but with physically unreasonable values for the parameters, in particular for the capacitance. In fact, Norford et al. (1985) found that to be the case for an office building. A general and systematic method based on Fourier analysis of extracting building parameters was given by Subbarao (1985); this method was shown by Norford et al. (1985) to yield more consistent parameters.

We shall now proceed with a definition of building capacitance based on Fourier analysis. Suppose the outdoor temperature is constant at $\bar{T}_{out}$ and solar radiation is zero. Then, if we impose electrical heat into the building given by Figure 2:

$$Q_{aux}(t) = \bar{Q}_{aux} + \Delta Q_{aux} \cos(2\pi f t) \tag{1}$$

then, under certain linearity assumptions, the resulting inside temperature behavior also is given in Figure 2:

$$T_{in}(t) = \bar{T}_{out} + \frac{\bar{Q}_{aux}}{L} + \frac{\Delta Q_{aux}}{V} \cos(2\pi f t - \phi_V) \; . \tag{2}$$

The quantities V, ϕ_V can be represented by a single vector $\vec{V}$ shown in the inset of Figure 2. For a massless building, $|\vec{V}| = L$ and $\phi_V = 0$. The $\vec{V}$-vector for the building is a sum of vectors representing individual components, with the component vectors modified by interaction factors to account for convection-radiation split (Subbarao and Anderson 1983).

Under conditions of constant outside temperature, no infiltration, no solar or internal gains, and auxiliary heat input given by Equation 1, the only quantity of interest is the resulting temperature and this is given by Equation 2. There is no need at this point to have a network representation; such a representation is needed only when nonsinusoidal driving functions are present. Nevertheless, let us represent the building by a network. Figure 1 gives such a representation only as far as the $\vec{V}$ admittance is concerned. Proper inclusion of the other admittances necessarily leads to a more complex circuit (Subbarao 1984). It is easy to show that

$$C_{in} = \frac{1}{2\pi f} \frac{|\vec{V} - L|}{\sin\theta} \tag{3}$$

$$U_{in} = \frac{|\vec{V} - L|}{\cos\theta} \tag{4}$$

where θ is the phase of $\vec{V} - L$.

Since $\vec{V}$ is a function of frequency, it follows that C_{in} and U_{in} are also functions of frequency. In general, this makes the network representation useless. However, for most

building components of interest, C_{in} has only a weak dependence on frequency over a wide range of frequencies. This also holds true for a wide range of buildings, with the diurnal frequency located in the plateau where C_{in} is changing slowly. In fact, this is the justification for the interpolation scheme of transfer functions given by Subbarao (1984). Thus, the above definition of C_{in} gives a useful and, as we shall see, measurable quantity.

The above discussion implies that the heat flow due to inside temperature fluctuations (over a wide range of frequencies) can be modeled in terms of a water container (namely, the lumped capacitance C_{in}) coupled to indoor air through a conductance U_{in}. The shape of the water container can be imagined appropriately to give the desired value of U_{in}.

The quantity that can be measured is the admittance $\vec{Y}$. We shall typically use $\vec{Y}$ in discussions of building capacitance, since $\vec{Y}$ has the useful property of being an element-by-element sum of individual $\vec{Y}$ vectors, with modifications resulting from the interaction factors. On the other hand, C_{in} of a building is not related in any simple way to individual capacitances (except in some limiting cases). For this reason, care is needed in interpreting the change in the effective capacitances of a building when some mass is added. Our discussion in terms of $\vec{Y}$ can be translated, if necessary, into a discussion in terms of C_{in} using Equation 3.

ISSUES IN MEASUREMENT OF BUILDING CAPACITANCE

The building capacitance was defined in Section 2 in terms of the inside temperature response to a sinusoidal heat input when outside temperature is constant, and solar radiation, infiltration, and incidental internal gains are absent. While a real building can be subjected to a sinusoidal heat input through computer-controlled electrical heaters, it is subject at the same time to variable ambient temperature, variable infiltration, solar radiation, and incidental gains. Furthermore, in the case of a residential building tested, there was a basement, and the heat flow to the basement must be properly treated. The effect of these "undesirable" influences can be subtracted using the following principle, which we shall call the signal enhancement principle.

The basic idea behind this principle is as follows: Suppose the building is monitored over two different periods such that the only major difference between the periods is in the addition of profiled heat input. The building response (more precisely the inside temperature) from period 1 can be used to determine what the building response would have been if the heat input in period 2 had remained approximately the same profile as in period 1. By subtracting this response from the actual response, we get the inside temperature in response purely to the additional profiled heat input. The effects of variations of outside temperature, solar radiation as well as unwanted variation of heat input, are all subtracted out. What remains is a strong signal for the building response to heat input only.

If all driving forces on the building (excepting the profiled gains) were identical in period 2 to those in period 1, then response data for period 1 could be directly subtracted from those data for period 2. To account for the inevitable variations between the periods, a model is necessary. For the case of a one-zone building coupled to a buffer space, a general linear model can be stated as

$$\int_{-\infty}^{\tau} \delta t' \left[\hat{Y}(t-t')\, T_{in}(t') - \hat{W}(t-t')\, T_{out}(t') \right. \tag{5}$$

$$\left. - \hat{W}_b(t-t')\, T_b(t') - \hat{S}(t-t')\, I_{sun}(t') \right] = Q_{int}(t) + Q_{aux}(t) \; .$$

In Equation 5, $\hat{Y}(t-t')$ is the time-domain form of the admittance defined in Equation 1 above. W, W_b, and S are similar transfer functions with respect to outside temperature, buffer space temperature, and solar irradiance, respectively.

In Equation 5, we have assumed auxiliary and internal gains to be instantaneous. (If not, they require their own transfer functions.) Variability of infiltration with stack and wind effects can be readily incorporated by defining an effective internal gain, which is the net gain after subtracting measured/modeled variable infiltration losses from normally defined internal gains. When the buffer space temperature is essentially a constant, $\int W_b(t-t')\, T_b(t')\, dt'$ can be replaced by $L_b\, T_b$. If there is no buffer space, L_b can be set to zero.

In order for Equation 5 to be manageable, it is essential to parameterize the various transfer functions to provide an adequate representation with as few parameters as possible. The following forms serve that purpose for a wide class of buildings (Subbarao 1984):

$$\hat{V}(t-t)' = (L_o+L_b)\,\delta(t-t') + U_{in}\left[\delta(t-t') - \frac{1}{\tau_{in}}\,e^{-(t-t)'/\tau_{in}}\right]$$

$$\hat{W}(t-t') = L_o\,\delta(t-t') - U_{out}\left[\delta(t-t') - \frac{1}{\tau_{out}}\,e^{-(t-t')/\tau_{out}}\right]$$

$$\hat{S}(t-t') = S_o\,\delta(t-t') = A_{sun}\left[\delta(t-t') - \frac{1}{\tau_{sun}}\,e^{-(t-t')/\tau_{sun}}\right]$$

$$\hat{W}_b(t-t') = L_b\delta\,(t-t')$$

where $\tau_{in} = U_{in}/C_{in}$ and $\tau_{out} = U_{out}/C_{out}$.

A justification for the above forms as well as for the relationship to Fourier transforms is given by Subbarao (1984).

The above signal enhancement principle plays a crucial role in accurate and repeatable determination of building capacitance. This is perhaps best explained through an example; this is done in the next section. The signal enhancement principle can be used in conjunction with any profile-step, impulse, sinusoidal, pseudorandom binary sequence or any other. In this article we concentrate on the sinusoidal profile for reasons discussed later.

If the quantities C_{in} and U_{in} show only weak dependences on frequency over a wide range of frequencies, we can choose the frequency of the sine wave to be at some convenient value located within the above range.

THERMAL MASS IN A SINGLE-FAMILY RESIDENCE

To demonstrate the measurements of thermal mass, data were taken in an unoccupied detached single-family residence, called the Maplewood house. The house has two natural thermal zones, an open, conditioned upstairs having a floor area of 115 m^2 (1240 ft^2), and an unfinished, totally open, unconditioned basement having an area of 103 m^2 (1110 ft^2). Temperature variation from room to room upstairs was typically less than 0.5°C, due to an open floor plan and use of two mixing fans. Insulated wood-frame wall and ceiling were nominally R12 and R32, respectively. The house has 15.5 m^2 (167 ft^2) gross glass area, with 11.8 m^2 (127 ft^2) on the south orientation. Although the house was largely unfurnished, some furnishings were present during the tests, including a large double bed, several chests of drawers, six large plants, an office desk, and several chairs. The upstairs conditioned space was treated as a single zone (mixing fans were used).

Performance data over a two-day period are shown in Figure 3. Infiltration was treated explicitly, using a model whose overall normalization was determined by a tracer gas decay. The model chosen was given by Sherman (1980):

$$ACH = \sqrt{b\Delta T + cv^2}\ . \qquad (7)$$

The ratio b/c was fixed to values recommended by Reinhold (1983). The results from the tracer decay were $b = 3.35 \times 10^{-3}\ {}^{o}C^{-1}$ ($1.86 \times 10^{-3}\ F^{-1}$), and $C = 3.51 \times 10^{-3}\ s^2/m^2$ ($0.70 \times 10^{-3}\ h^2/mi^2$). Infiltration flow was calculated hourly from this model and subtracted from or added to internal gains (due to refrigerator, light, etc.); the resulting effective internal gains are plotted in Figure 3.

Table 1 shows two of the many possible sets of values for the nine model parameters, regressed from the first two days of data of Figure 3. Both parameter sets predict the measured temperature with an rms error of 0.1°C (0.2 F). (The inside temperature predicted by the two sets and the measured inside temperature--all three curves are practically indistinguishable on the scale of Figure 3.) Parameter set 1 implies a factor of ~2 higher heat loss from the living space to the outside and to the basement; but this is compensated for by the higher solar gains implied by the set 1 (again nearly a factor of 2). The higher storage in set 1 and the coupling to storage are all such that the net effect on inside air temperature is the same. The quantity of central interest in this article is the effective thermal capacitance C_{in}. This is 7725 Btu/F in set 1 and 2202 Btu/F in set 2. The first two days of data in Figure 3 thus give a very poor estimate of C_{in}. The fact that a model "fits" a given data set is no guarantee that the model or its parameters are "correct." We now show that

data from a second time period with sinusoidal variation of internal heat significantly reduce the uncertainty in the value.

During a second time period, an extra heat (W) of

$$\dot{Q}_{prof} = 1899.6 - 1834.1 \sin \frac{2\pi}{16} (t - 0.869) \quad (8)$$

was introduced into the building. This has a period of 16 h; this was chosen to be far enough away from 24 h to avoid confounding effects due to strong diurnal components in natural driving functions, but close enough to be of relevance (through suitable extrapolation) to the diurnal cycle. The data for period 2 are also given in Figure 3. If the first set is used for subtraction for period 2, the resulting temperature response is shown in Figure 4. This can be fit very well to

$$12.4 - 2.133 \sin[\frac{2\pi}{16} (t - 2.972)] , \quad (9)$$

in ^{o}C, with a residual standard deviations of $0.22^{o}C$ (0.39 F). The smallness of this residual confirms the validity of the linearity assumption.

From the above, we see that from the definition of $\vec{V}$:

$$|\vec{V}| = 1834.1 \text{ W}/2.133^{o}C$$

$$= 860 \text{ W}/^{o}C ,$$

and phase of $\vec{V}$ is 2.972 - 0.869 = 2.103 h. Thus, $\vec{V} = 860|\underline{47.3^{o}}$ W/^{o}C (1630 $|\underline{47.3^{o}}$ Btu/h F).

If we use the second set of circuit parameters from Table 1, a similar analysis gives an inside temperature response of

$$12.7 - 2.072 \sin[\frac{2\pi}{16} (t - 2.965)] , \quad (10)$$

in ^{o}C, with a residual standard deviation of $0.46^{o}C$ (0.83 F).

As before, this gives

$$|\vec{V}| = 885 \ |\underline{47.2} \text{ W}/^{o}C \ (1670 \ |\underline{47.2^{o}} \text{ Btu/h F}) . \quad (11)$$

Thus, even though the two sets of circuit parameters are so dramatically different, when used for subtraction through the signal enhancement principle, the resulting estimates of $\vec{V}$ are very close (±1.2% in magnitude).

We have used a sinusoidal profile for known heat input. Other forms such as step functions and square waves are perhaps easier from an experimental point of view. While experimental ease is an important consideration, there are distinct theoretical advantages for sine waves:

1. For a linear system, the response to a sine wave is a sine wave of the same frequency. The goodness of the fit to sine wave of the output is an approximate measure of the validity of the linearity approximation. Thus sine wave profile provides a self-test.

2. Sine waves at different frequencies are approximately orthogonal over finite time intervals. Thus any errors in subtracting the behavior at the other frequencies (especially at the strong diurnal frequency) have only small effect on the admittance estimates. Thus the $\vec{V}$ admittance at 16 h is a very robust estimate.

The value $\vec{V}$ (16 h) = 860 $|\underline{47.3^{o}}$ W/^{o}C (1630 $|\underline{47.3^{o}}$ Btu/h F) along with $L + L_b \simeq 317$ W/^{o}C (600 Btu/h F) (obtained independently) gives an effective capacitance of 7057 kJ/^{o}C (3716 Btu/F) coupled to inside air through a conductance of 1772 W/^{o}C (3359 Btu/h F). Strictly speaking, these numbers are only true for the 16-h cycle. But practically, they are adequate for a range of frequencies around the 16-h cycle including the diurnal cycle; they are very likely to be incorrect for very low and very high frequencies.

It is of interest to compare the measured value of the mass parameter with a prediction based on the plans and handbook values for thermophysical properties. Results of the calculation are shown in Figure 5. Note that the measured value is significantly larger than the calculated value. This is because of:

-- furniture, etc., not included in the calculation

-- deviation of actual and handbook values for thermophysical properties

-- use of a combined radiation/convection coefficient in calculations

TEST CELL INTERNAL MASS ADDITION

A good test of the method discussed in earlier sections for measuring building capacitance is its ability to determine changes due to addition of masses. Measurements were made in a room-sized test cell before and after mass was added to the cell interior. The additional mass was chosen as 80 L (21 gal) of water, allowing a simple model to be used in estimating expected change in the mass parameters. The before and after tests will confirm both the accuracy and physical interpretation of the parameters if the expected change agrees with the measured change.

The test cell is located at the Solar Energy Research Institute (SERI) test site in Golden, CO. Cell interior height is 2.47 m, and floor interior dimensions are 1.66 m × 2.77 m, with the long dimension oriented north-south. Average insulation level is about R10 over all exterior opaque surfaces. Tracer gas decay tests indicated a leakage rate of ~0.2 ACH; hence infiltration was not explicitly modeled. The south-facing aperture (gross dimensions 2.47 m × 1.65 m) is fitted with eight double-pane window units, with net clear glazing area of ~2.3 m^2. The mullions are unfinished pine wood, and extend ~12 cm beyond the inner pane. The floor is covered with bricks 5.7 cm thick. For the second test, extra thermal capacitance was added by placing four 20-L plastic bottles in the cell. The bottles were placed on the cell floor near the north wall.

Tests were designed according to Subbarao et al. (1985), consisting of specifying: 1) the measured channels, and 2) the internal gains profiles. For these tests, we have:

1. Data channels: T_{in}, T_{out}, I_{sun}, and Q_{int}.

2. Internal gains profiles: Two periods, approximately two days each.

   -- During the first period, heat input from the electric heaters was chosen to be zero.

   -- During the second period, electric heat was introduced as $Q_{prof} = \bar{Q} + \Delta Q \sin [\omega (t+t_o)]$, with $\bar{Q}$ ~ 225 W, and ΔQ ~ 225 W.

Data for the test cell without the water jugs are shown in Figure 6. Notice the sinusoidal profile on the internal gains in Figure 6, which is the key feature leading to the precise determination of the mass parameters. The data were analyzed to extract the value of $\vec{V}$ (T = 16 h), along with other descriptive parameters. The result for the mass parameter $\vec{V}$ was

$$\vec{V}_b = 63.1 \; |\underline{31.4}^o \text{ W/}^o\text{C} \; (119.6 \; |\underline{31.4}^o \text{ Btu/h F}) \; . \tag{12}$$

A similar experiment two months later gave $\vec{V} = 63.0 \; |\underline{32.1}^o$ W/°C (119.4 $|\underline{32.1}^o$ Btu/h F) showing high repeatability (<1%) under different conditions of T_{out} and Q_{sun}.

The protocol was repeated (see Figure 7) after 80 L of water were added to the cell interior. As can be seen by comparing Figure 6 with Figure 7, the data are qualitatively similar to the before case, with no intuitively obvious "signal" for the mass increment. The result for $\vec{V}$ was:

$$\vec{V}_a = 72.7 \; |\underline{27.8}^o \text{ W/}^o\text{C} \; (137.9 \; |\underline{27.8}^o \text{ Btu/h F}) \; . \tag{13}$$

We thus determine

$$\Delta\vec{V}_{meas} = \vec{V}_a - \vec{V}_b = 10.6 \; |\underline{5.7}^o \text{ W/}^o\text{C} \; (20.2 \; |\underline{5.7}^o \text{ Btu/h F}) \; . \tag{14}$$

The difference $\Delta\vec{V}_{meas}$ is due to the incremental mass and the effect of the water containers (four 5-gal, round, polyethylene jugs) on radiative-convective couplings. If we ignore the (presumably small) second effect, we can compare a calculated value based on a simple isothermal one-node model, as in Figure 8. It is easy to show that

$$\Delta\vec{V}_{calc} = U_w\sqrt{1 + 1/(\omega\tau)^2}\ \underline{|\tan^{-1}(\omega\tau)}^{-1}. \quad (15)$$

If assumptions are made as in Table 2, then we calculate

$$\Delta\vec{V}_{calc} = 13.5\ \underline{|21.7^o}\ W/^oC\ (25.5\ \underline{|21.7^o}\ Btu/h\ F)\ . \quad (16)$$

Calculations are uncertain by about 25%, mainly due to uncertainty in the combined film coefficient assumed and the complicated geometry and view factors for the water jugs. The agreement between measured and calculated quantities is reasonable.

DISCUSSION

As seen earlier, the thermal admittance can be measured accurately and repeatedly. As shown for the Maplewood residence, this has diagnostic applications; namely, comparing measured and calculated values of this admittance. However, this does not allow us to determine the building element(s) responsible for any difference. This is quite analogous to measuring the building loss coefficient for diagnostic applications: if the measured and calculated loss coefficients do not agree, we can assess the impact of this on the building performance, but we cannot determine the element(s) responsible for the difference. The impact on consumption, temperature swings, etc., of the difference between measured and calculated admittance can be assessed through "macrodynamic" simulations implemented through BEVA, as described by Subbarao (1985). The designer thus determines whether performance differs from that predicted during design because the calculated descriptive inputs differ from the actual, or because driving forces differ from those assumed during design (weather, schedules, etc.).

Another application is in providing measurement-based characterization of furnishings in a building. It is in general very difficult to make such estimates from first principles. One does not have reliable values for effective film coefficients in such torturous geometries as couches, chairs, beds, plants, etc. There are many layers of materials and so on. Further, it is very tedious (at best) to estimate the impact of furnishings on infrared interactions. However, all of these complexities are subsumed into a measurement of the $\vec{V}$ before and after furnishings are added to a house.

CONCLUSION

It has been demonstrated that short-term data must be appropriately profiled to reduce the error in measurement of the internal mass. Several days of data with small internal gains, even with significant variation in the internal temperature, are inadequate for determining $\vec{V}$. However, when the test is augmented with an additional period with sinusoidal variation of Q_{in}, the value was apparently quite well-determined.

Two examples have been given. In the case of the test cell, a known mass addition was measured as a before and after difference in parameters, a stringent test of accuracy. In the case of the residence, it was shown that a reasonably detailed calculation of thermal admittance differed significantly from the measured value. Part of the deviation is due to neglect of furnishings. The designer thus has available a means for determining whether deviations between predicted and actual performance of the building are due to thermal description deviations (i.e., measured parameters differ from calculated) or from other sources (i.e., occupancy, weather, etc.).

NOMENCLATURE

A	area
ACH	air changes per hour
b	stack factor in infiltration model
c	wind factor in infiltration model
C	thermal capacitance

f	frequency
I	irradiance
L	building load coefficient
Q	thermal energy
S_o	effective solar area
$\hat{S}$	solar radiation transfer function
t	time
T	temperature or period
U	U-value of thermal coupling between internal mass and air node
$\hat{V}$	indoor temperature transfer function
$\hat{\vec{V}}$	indoor temperature transfer function at diurnal frequency
$\hat{W}$	outdoor temperature transfer function
v	wind velocity

Greek

Δ	change in
σ	standard deviation
ω	angular frequency

Subscripts

aux	auxiliary
b	basement or buffer space
in	inside
int	internal gains
out	outside
sun	solar radiation
w	water

REFERENCES

Kelley, M.E.; Duffy, J.; and Slote, J.K. 1984. "Rapid measurement of time constant for performance prediction and design," Proceedings 9th Passive Solar Conference, ASES.

Norford, L.K.; Rabl, A.; Socolow, R.H.; and Persily, A.K. 1985. "Measurement of thermal characteristics of office buildings," presented at ASHRAE Conference, Thermal Performance of Building Envelopes, Dec. 2-5.

Reinhold, C.; and Sonderegger, R. 1983. Component leakage areas in residential buildings, LBL-16221.

Sherman, M.; and Grimsrud, D. 1980. Measurement of infiltration using fan pressurization and weather data, LBL-10852.

Sonderegger, R.C. 1978. "Diagnostic tests determining the thermal response of a house." ASHRAE Transactions, Vol. 84, No. 1.

Subbarao, K. 1984. BEVA (building element vector analysis)--a new hour-by-hour building energy simulation with system parameters as inputs, SERI/TR-254-2195, Golden, CO: Solar Energy Research Institute.

Subbarao, K. 1985. Thermal parameters for single and multizone buildings and their determination from performance data, SERI/TR-253-2617, Golden, CO: Solar Energy Research Institute.

Subbarao, K.; and Anderson, J. 1983. "A graphical method for passive building energy analysis," Tran. ASME, Vol. 105.

Subbarao, K.; Mort, D.; and Burch, J. 1985. Short-term measurements for the determination of envelope retrofit performance, SERI/TP-253-2639, Golden, CO: Solar Energy Research Institute.

ACKNOWLEDGMENTS

We gratefully acknowledge the support of this work by the U.S. Department of Energy, Office of Buildings and Community Systems, Building Services Division. The capable assistance of Don Frey & Brad Collins (AEC Corporation) is acknowledged in experiment design and data acquisition. Rob deKieffer is most warmly thanked for helping in many ways.

TABLE 1

Maplewood House Parameters

Two sets of building parameters that give practically indistinguishable performance ($\sigma_1 \sim \sigma_2 \sim 0.1^{\circ}C$) under the driving functions of Figure 3:

	Parameter Set 1		Parameter Set 2	
L ($W/^{\circ}C$ [Btu/h F])	184	(349)	82	(156)
L_B ($W/^{\circ}C$ [Btu/h F])	271	(513)	215	(407)
S_o (m^2)	7.7	(82.7)	4.2	(45.0)
U_{in} ($W/^{\circ}C$)	2,081	(3,945)	2,977	(5,643)
C_{in} ($kJ/^{\circ}C$ [Btu/F])	14,670	(7,725)	4,185	(2,204)
U_{out} ($W/^{\circ}C$)	108	(205)	39	(73)
C_{out} ($kJ/^{\circ}C$ [Btu/F])	334	(176)	144	(76)
A (m^2 [ft^2])	6.5	(70.2)	3.1	(33.6)
τ (h)	3.4		11.1	

TABLE 2

Parameters Assumed for $\Delta\vec{V}$ Calculation

Coupled area, A	3.6 m^2 (39.1 ft^2)
Combined film, h	4.0 $W/^{\circ}C\ m^2$ (0.7 Btu/h ft^2 F)
Total coupling, U = hA	14.4 $W/^{\circ}C$ (27.4 Btu/h F ft^2)
Total mass, C	332 $kJ/^{\circ}C$ (174.9 Btu/F)
Time constant, τ = C/U	6.4 h
$\omega\tau = \frac{2\pi}{16\ h} \cdot \tau$	2.51

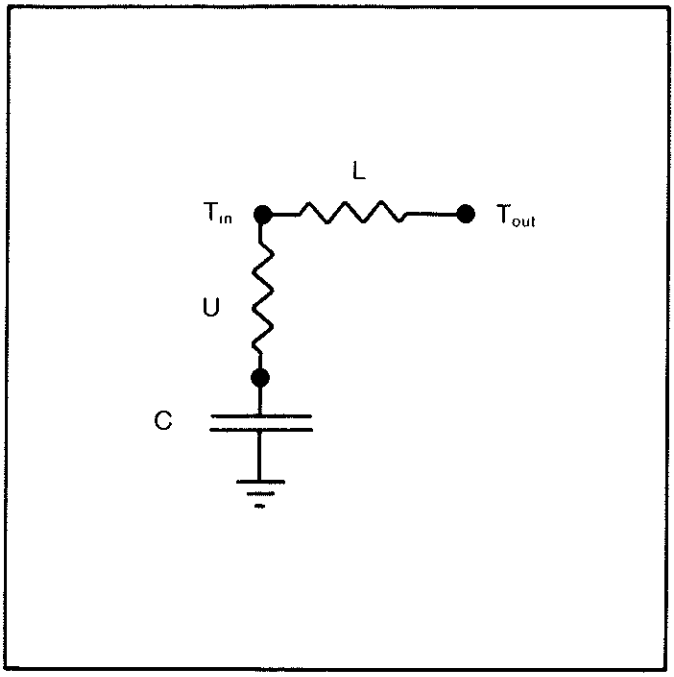

Figure 1. Simple building model. A simple thermal circuit is shown, which includes a capacitance for internal mass. There is only a steady-state coupling to outside air

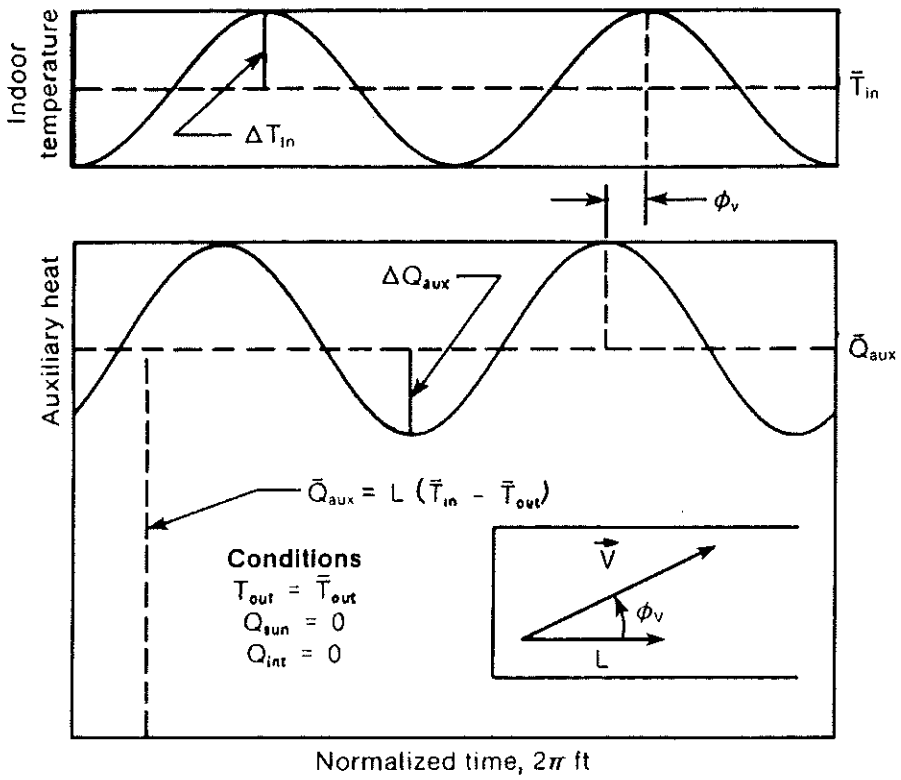

Figure 2. Definition of $\vec{V}$ admittance. The $\vec{V}$ admittance is defined in terms of sinusoidal temperature response to sinusoidal addition of heat to the interior air of the building

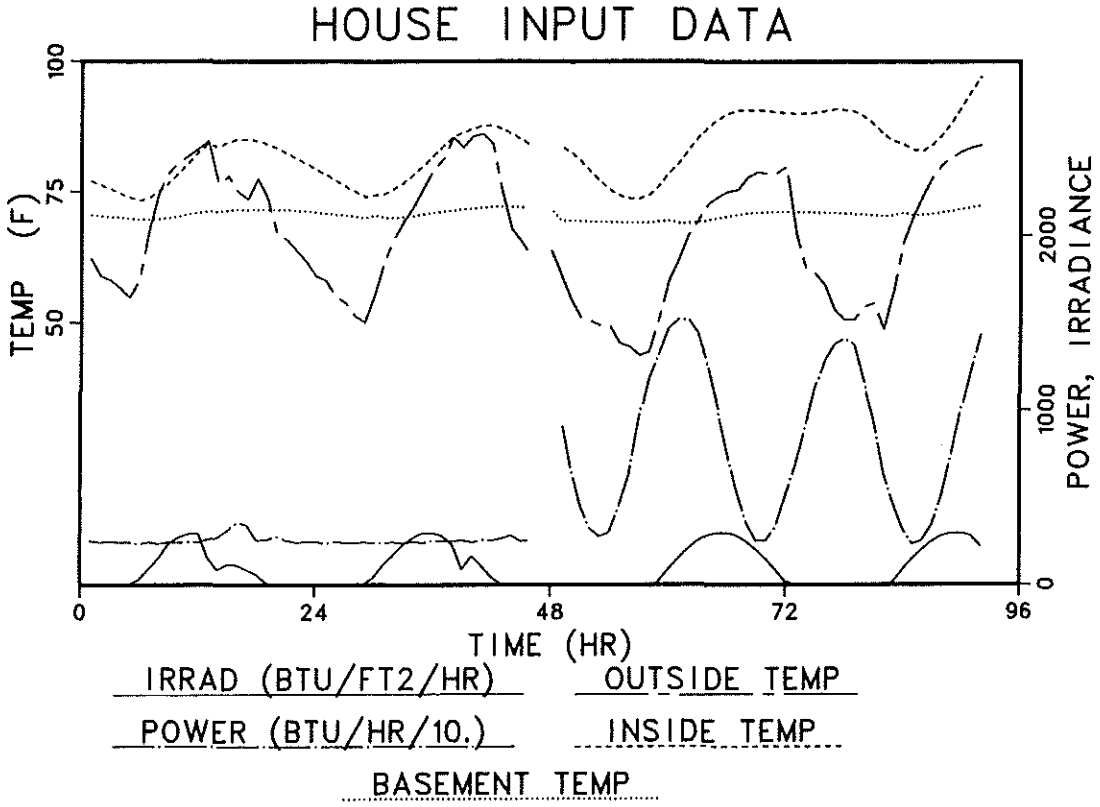

Figure 3. House input data. A graph of the macrodynamic data channels--inside temperature, outside temperature, basement temperature, solar radiation, and effective internal gains--is given for two

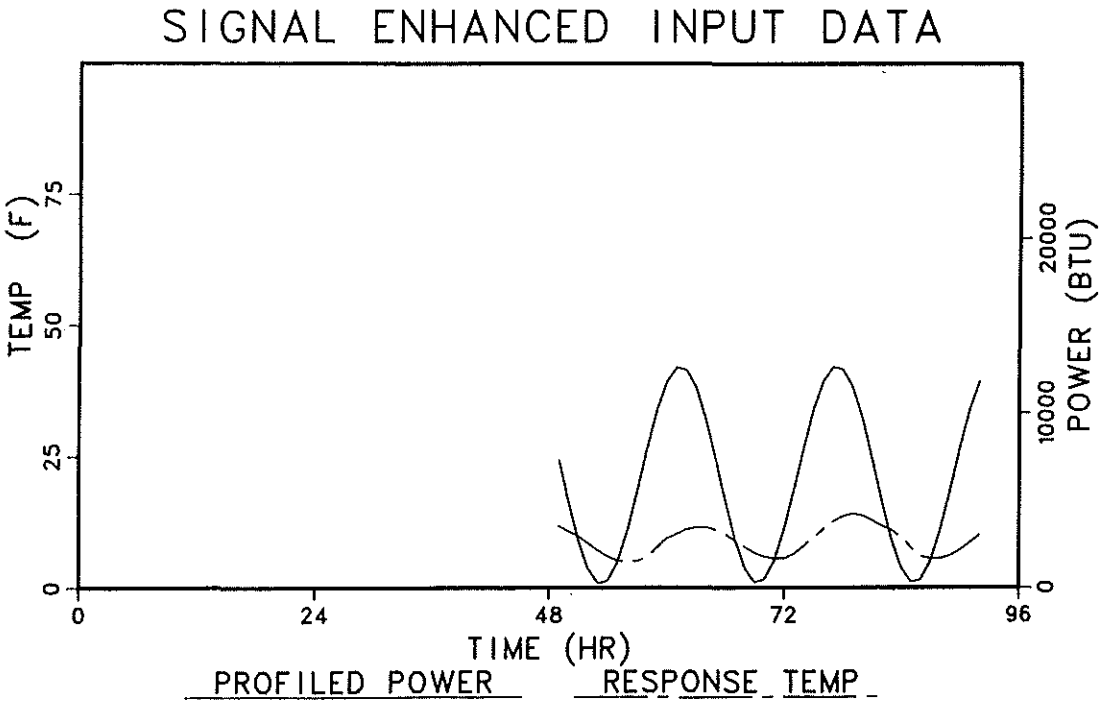

Figure 4. Signal-enhanced input data. The inside temperature (output) in response to a purely sinusoidal heat input is a direct measurement of the $\vec{V}$ admittance. All other effects have been subtracted out using the parameters in column 1 of Table 1

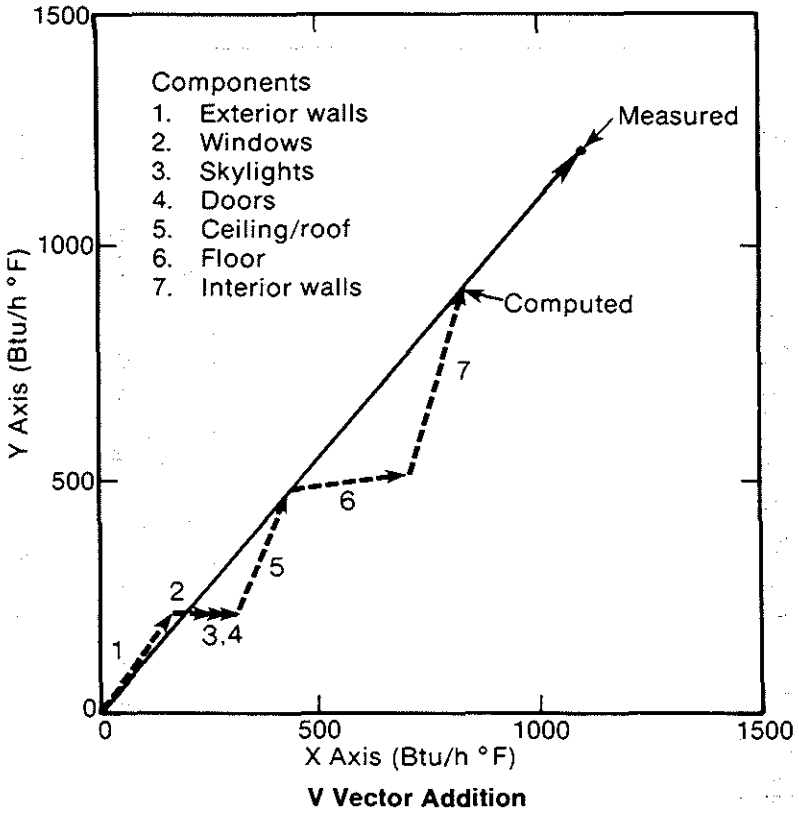

Figure 5. V vector addition. A plot of the element-by-element vector sum for the calculation of V is given. The long vector is that obtained from measurements

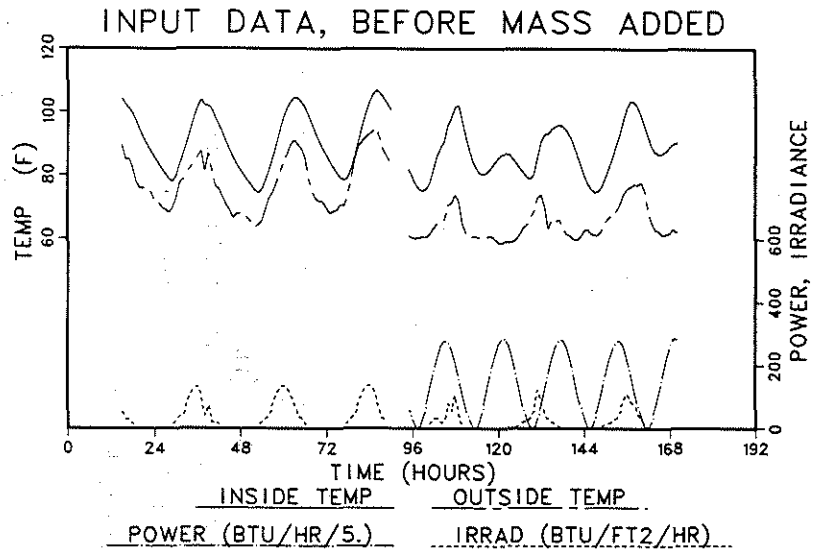

Figure 6. Input data, before mass added. The four data channels--inside temperature, outside temperature, solar radiation incident on vertical south, and internal gains--are shown over a seven-day period

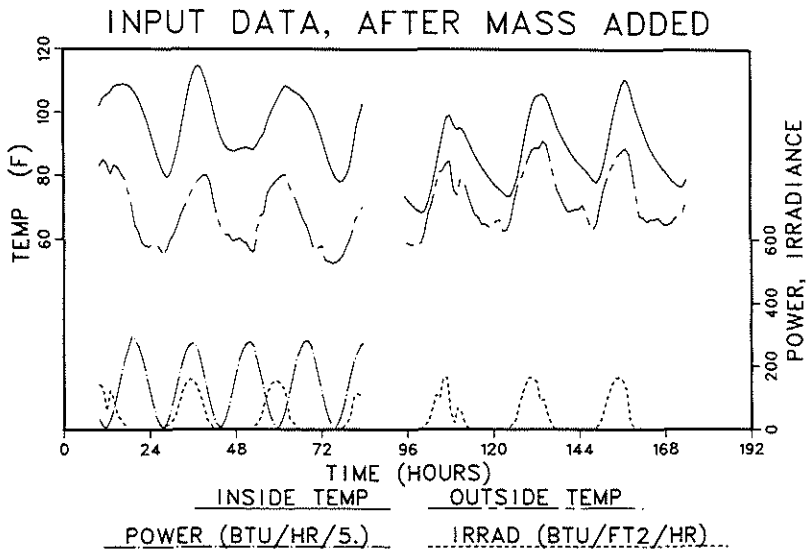

Figure 7. Input data, after mass added. The four data channels--inside temperature, outside temperature, solar radiation, incident on vertical south, and internal gains--are shown over a seven-day period

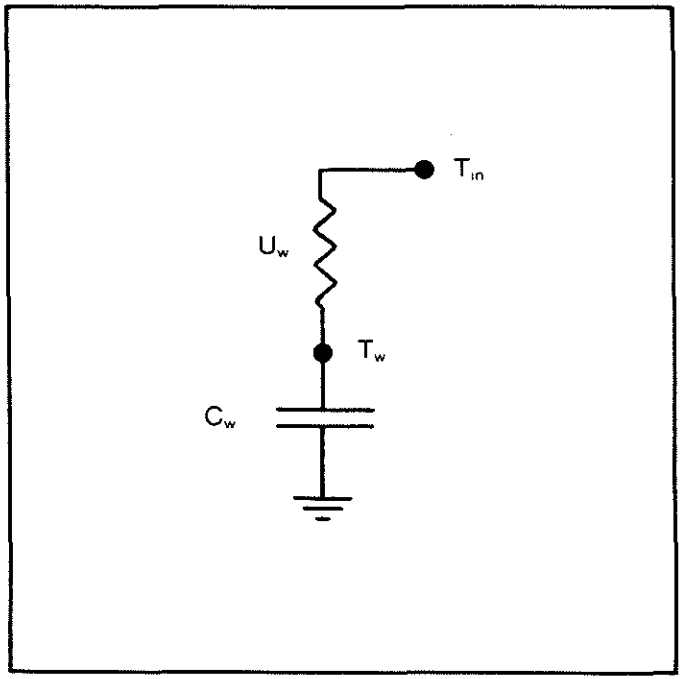

Model for Added Water

Figure 8. Model for added water. A simple thermal circuit is shown for calculation of $\bar{V}$, with neglect of interaction factors